Supplementary Figure 1

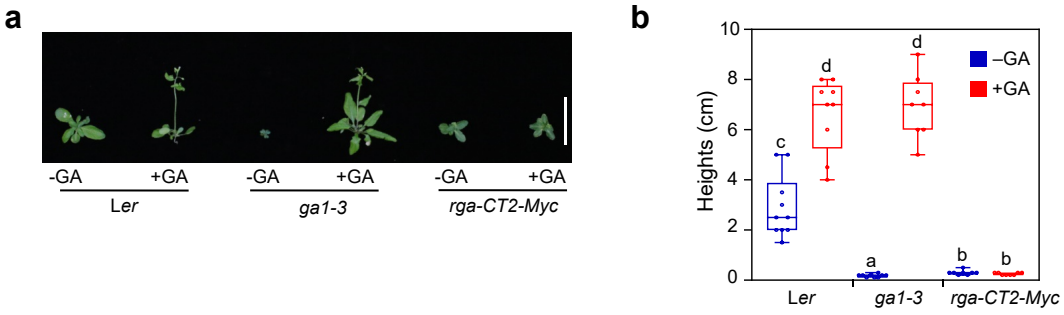

Supplementary Figure 1. P_{RGA}*:rga-CT2-Myc* conferred GA-unresponsive dwarf phenotype. **a**, Representative 34-d-old L*er* (WT), *ga1-3* and a P_{RGA}*:rga-CT2-Myc* line after weekly treat ments with 100 μM GA_3 (+) or mock (–) as labeled. Bar = 5 cm. **b**, Boxplot showing plant heights of different lines as labeled. n ≥ 8. Different letters above bars represent significant differences, $p < 0.05$. Statistical analyses were performed with two-tailed Student's t tests. Center lines and box edges are medians and the lower/upper quartiles, respectively. Whiskers extend to the lowest and highest data points within 1.5× interquartile range (IQR) below and above the lower and upper quartiles, respectively. Exact n and *p* values were listed in Supplementary Data.

Supplementary Figure 2

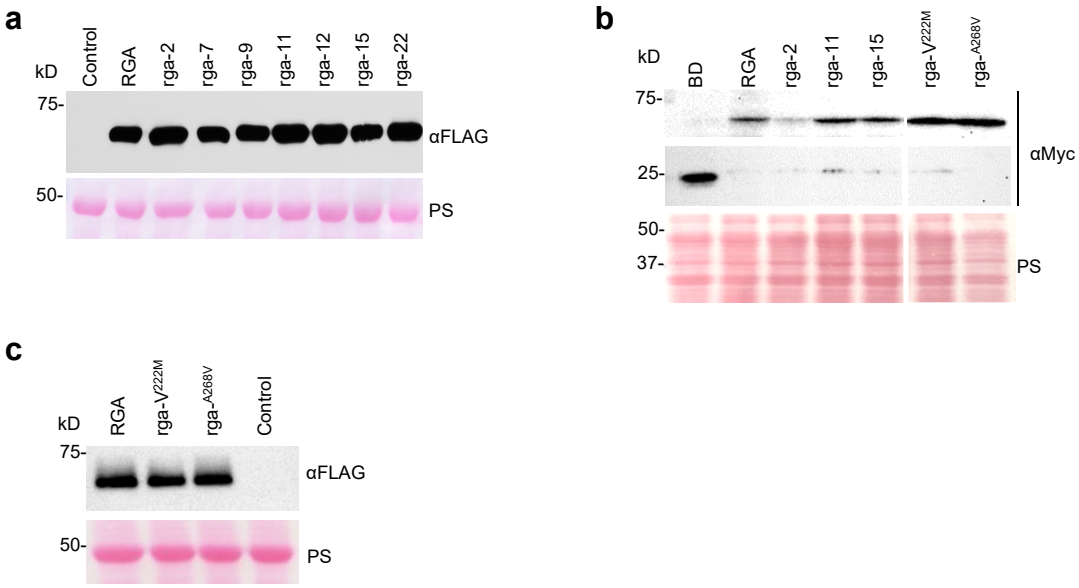

Supplementary Figure 2. Detection of RGA and rga proteins in Y2H and dual luciferase assays. **a** and **c**, FLAG-RGA/rga proteins in *N. benthamiana* extracts were detected by immunoblot analysis using an anti-FLAG antibody. Ponceau S (PS) stained gel images showing similar sample loading. **b**, Myc-Gal4 BD-RGA and -rga proteins in yeast extracts were detected by immunoblot analysis using an anti-Myc antibody. Ponceau S (PS) stained gel image showing similar sample loading. Levels of rga-11 and rga-15 were similar to RGA, rga-2 was lower than RGA, and rga^{V222M} and rga^{A268V} were higher than RGA. The lower amounts of rga-2 may contribute to the reduced growth of rga-2 + IDD3 in comparison to other rga proteins. In **a**-**c**, representative images of two biological repeats are shown. Unprocessed gel blot images are in Supplementary Figure 11.

Supplementary Figure 3

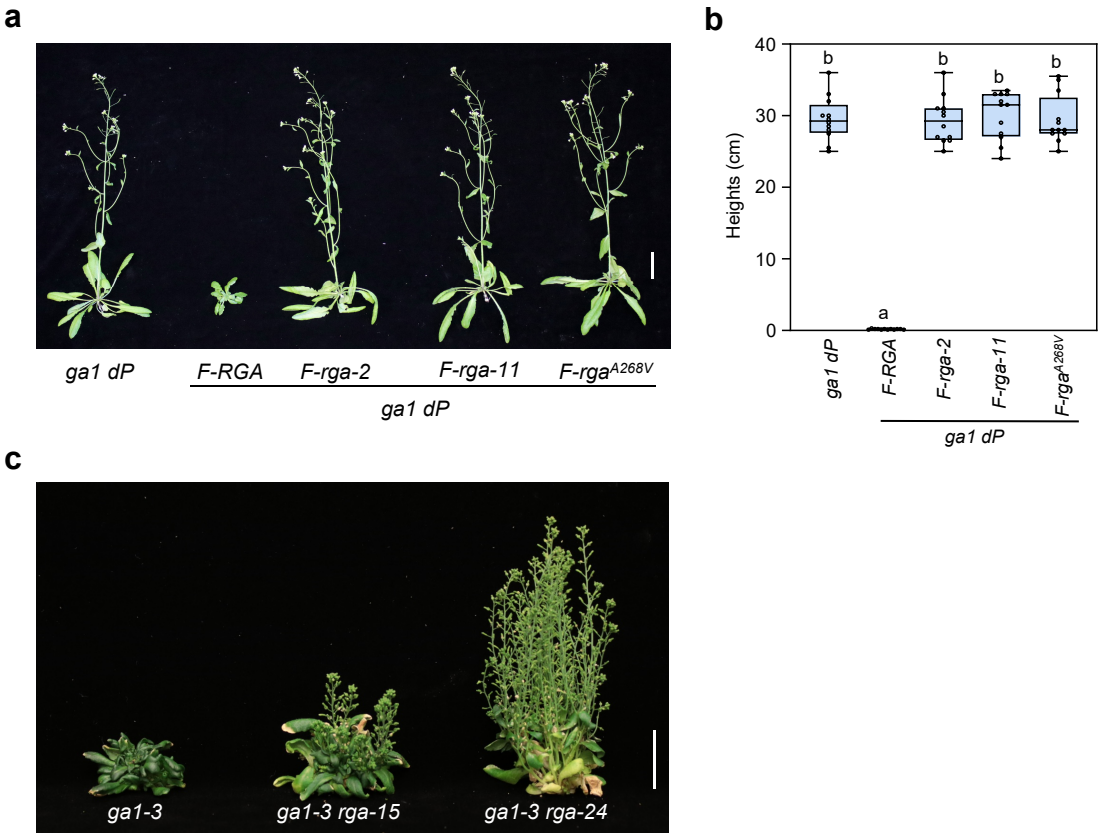

Supplementary Figure 3. Phenotypes of *ga1 rga-15* and transgenic lines expressing *FLAG-RGA* or different *FLAG-rga*. **a**, Phenotypes of P_{RGA}*:FLAG-rga-2, -rga-11* and *-rga*^{A268V} *ga1 dP* transgenic lines were similar to *ga1 dP*, whereas P_{RGA}*:FLAG-RGA* in *ga1 dP* restored the dwarf phenotype. All plants were 41-d-old under LD conditions. Bar = 5 cm. **b**, Boxplot showing plant heights of different lines as labeled. n = 12. Different letters above bars represent significant differences, $p < 0.01$. Statistical analyses were performed with two-tailed Student's t tests. Center lines and box edges are medians and the lower/upper quartiles, respectively. Whiskers extend to the lowest and highest data points within 1.5× interquartile range (IQR) below and above the lower and upper quartiles, respectively. Exact n and *p* values were listed in Supplementary Data. **c**, *rga-15* only mildly rescued the dwarf phenotype of *ga1-3* in comparison to the null *rga-24* allele. Representative 83-d-old *ga1-3* (with *RGA*) and *ga1 rga* mutants as labeled. Bar = 2 cm.

Supplementary Figure 4

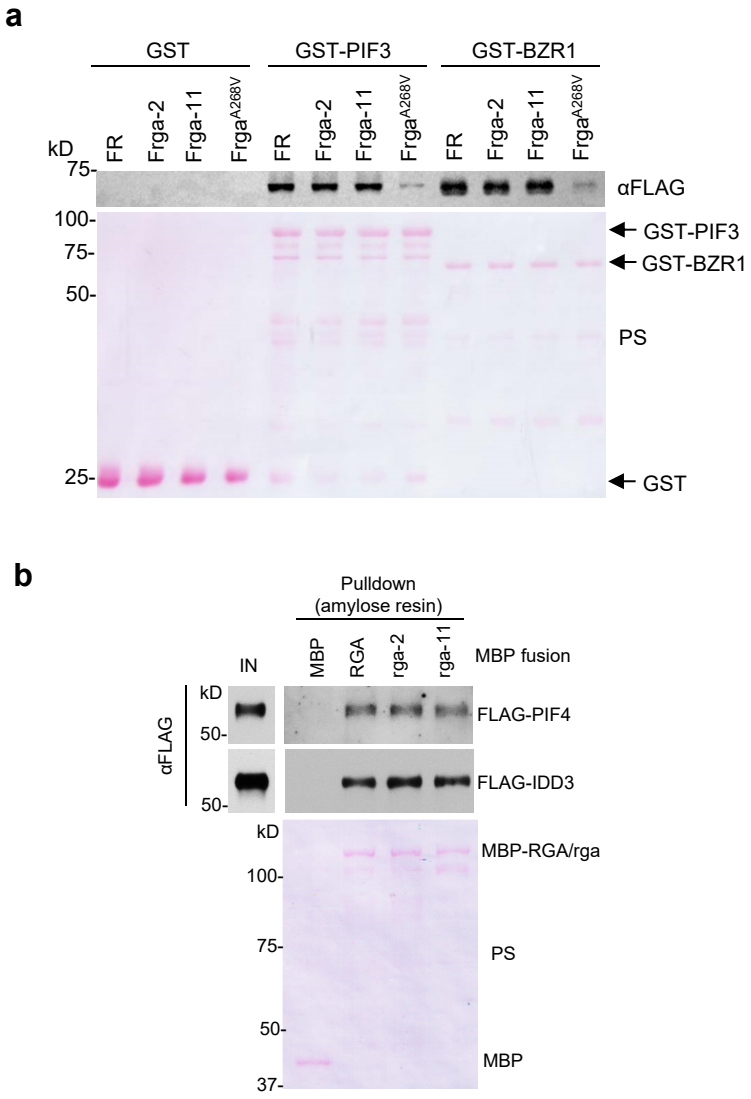

Supplementary Figure 4. In vitro pulldown assays to examine RGA/rga interaction with TFs. a, The images of Ponceau S-stained blots show the GST and GST-BZR1, GST-PIF3 proteins used in the pull-down assays in Fig. 4a. **b**, In vitro pulldown assay. Recombinant MBP, MBP-RGA, MBP-rga-2, MBP-rga-11 bound to amylose resin were used separately to pull down FLAG-PIF4 or FLAG-IDD3 from protein extracts from *N. benthamiana*. Immunoblots containing input plant extracts and pulldown samples were detected with an anti-FLAG antibody. Ponceau S (PS)-stained blots indicated that similar amounts of the MBP/MBP-fusion proteins were used in each set of the pulldown assays. In **a**-**b**, representative images of three (in **a**) or two (in **b**) biological repeats are shown. Unprocessed gel blot images are in Supplementary Figure 11.

Supplementary Figure 5

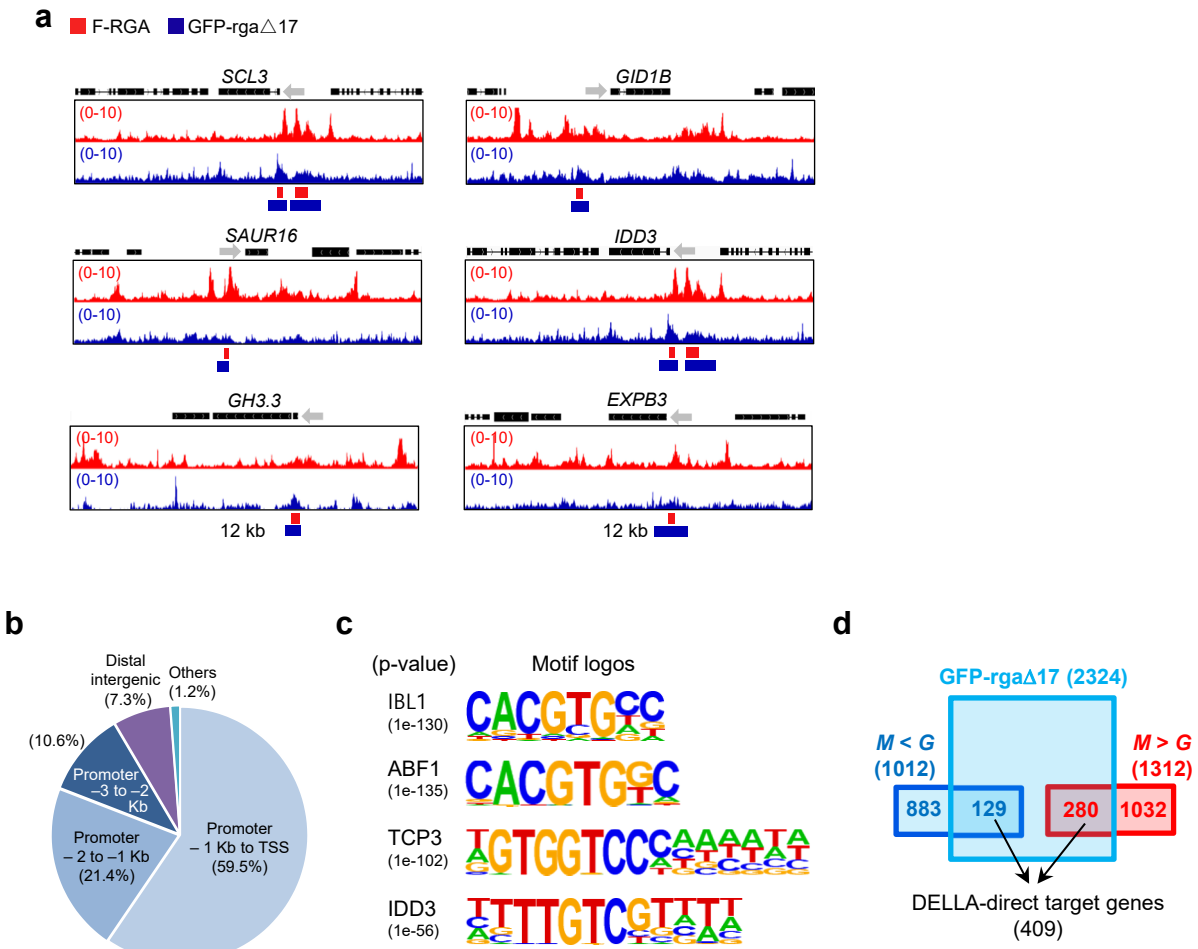

Supplementary Figure 5. Additional ChIP-Seq data. a, Genome browser views of F-RGA and GFP-rgaΔ17 ChIP-seq binding profiles at selected loci (12 kb region is shown in each panel). Gene structures and names are above each panel. Red bars and blue bars below indicate F-RGA and GFP-rgaΔ17 binding peaks, respectively. The data range of y-axis is 0-10. **b**, Genomic distribution of FLAG-RGA binding peaks. Promoter regions [–3 kb to transcription start site (TSS)] were divided into three segments as labeled. Others include exon, intron, downstream and 3' UTR. **c**, Most highly enriched *cis*-elements for IBL1 (bHLH), ABF1 (bZIP), TCP3 (TCP), IDD3 (IDD) near the binding peaks of FLAG-RGA. **d**, RGA-direct target genes based on overlapping genes between genes located near a GFP-rgaΔ17 peak and GA-responsive genes (based on an RNA-seq dataset[37]) (see Methods for detail). M, mock treatment. G, GA treatment. M < G (GA-upregulated genes) and M > G (GA-downregulated genes). RGA acts as 'direct repressor' and 'direct activator' on 129 and 280 genes, respectively. The list of all RGA-direct target genes is in **Supplementary Table 3**.

Supplementary Figure 6

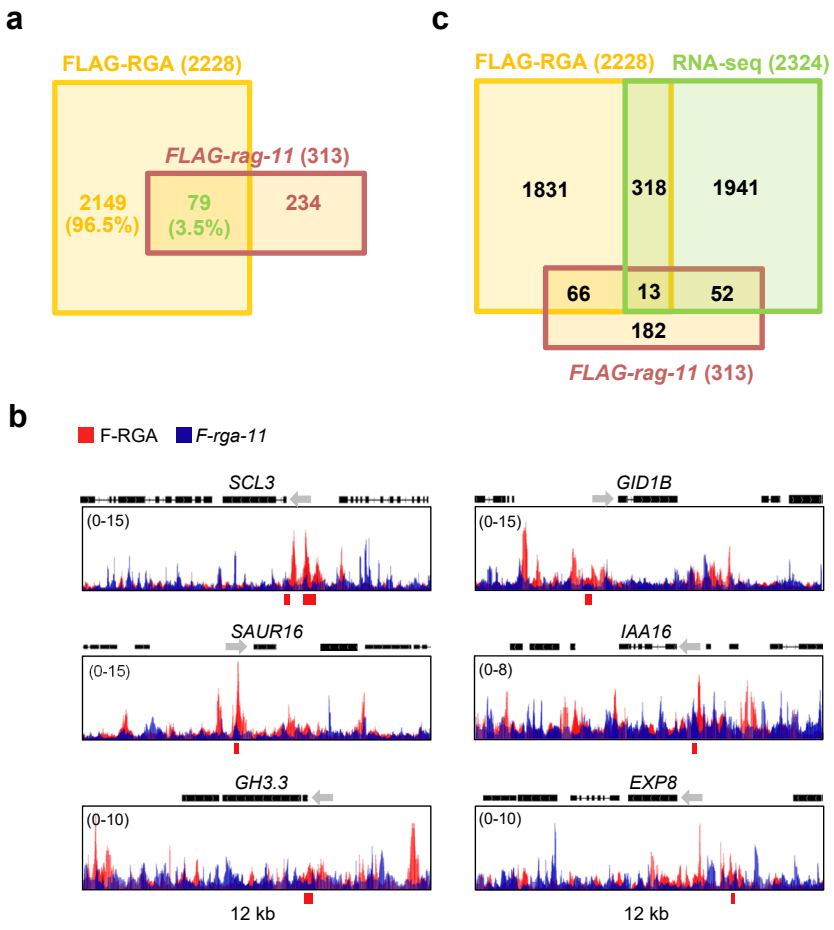

Supplementary Figure 6. FLAG-rga-11 showed much reduced chromatin binding in comparison to F-RGA by ChIP-seq analysis. a, Venn diagram showing the overlap between genes adjacent to the binding sites of F-RGA and F-rga-11. **b**, Genome browser views of F-RGA and F-rga-11 ChIP-seq binding profiles at selected RGA target genes (12 kb region is shown in each panel). F-RGA and *F-rga-11* tracks are overlaid. Red bars below indicate differential RGA binding peaks. The data range of y-axis as shown in the left corner of each image. **c**, A Venn diagram showing the overlap among genes adjacent to the binding sites of F-RGA, F-rga-11, and GA-responsive genes (based on an RNA-Seq dataset[37]).

Supplementary Figure 7

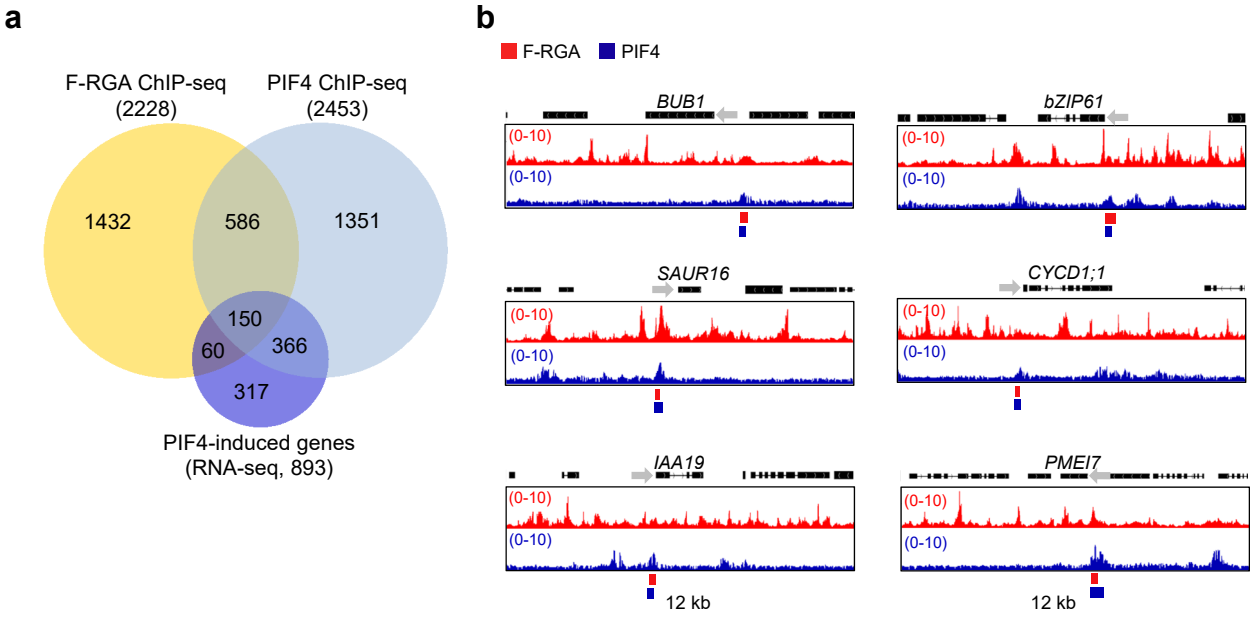

Supplementary Figure 7. High degree of co-localization of RGA and PIF4 binding peaks associated with PIF-induced genes. a, Venn diagram showing the overlap among genes adjacent to the binding sites of FLAG-RGA (this study), PIF4 (ChIP-seq dataset[53]) and PIF4-induced genes (RNA-seq dataset[53]). **b**, Genome browser views of FLAG-RGA and PIF4 binding peak regions at selected genes. Gene structures and names are shown above each panel. Red bars and blue bars below the panels indicate F-RGA and PIF4 binding peak regions, respectively. Data range as shown in the left corner of each image.

Supplementary Figure 8

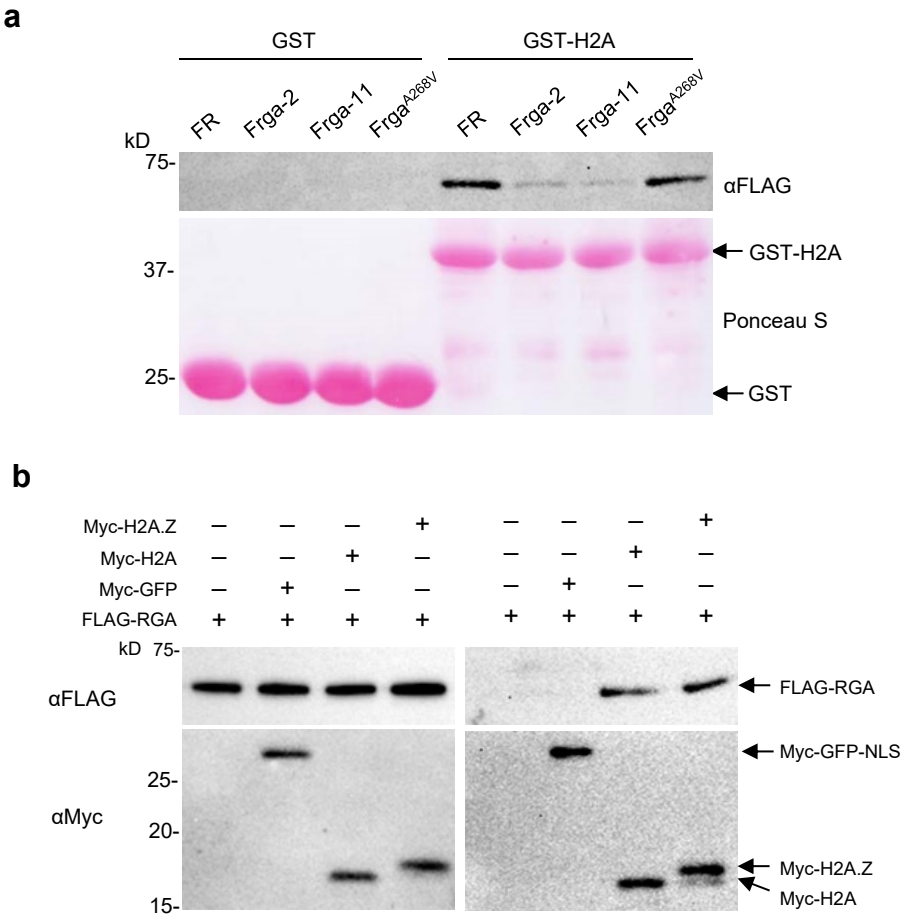

Supplementary Fig. 8. Pull-down and co-IP assays. a, The image of Ponceau S-stained blot shows the GST and GST-H2A proteins used in the pull-down assays in Fig. 7c. **b**, Co-IP assay showing RGA interacts with H2A and H2A.Z similarly. FLAG-RGA was expressed alone or co-expressed with Myc-H2A, Myc-H2A.Z or Myc-GFP-NLS in *N. benthamiana* as indicated. An anti-Myc antibody was used for IP, and protein blots were probed with anti-Myc and anti-FLAG antibodies, separately. In **a**-**b**, representative images of three (in **a**) or two (in **b**) biological repeats are shown. Unprocessed gel blot images are in Supplementary Figure 11.

Supplementary Figure 9

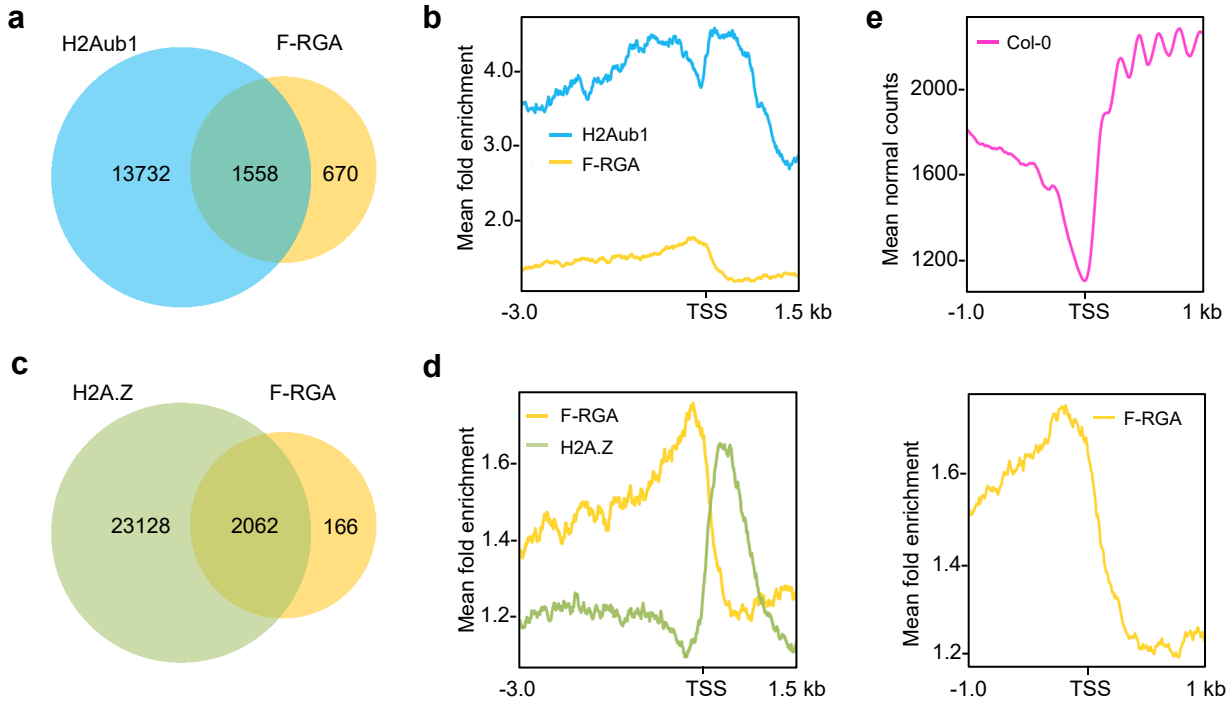

Supplementary Figure 9. Genome-wide RGA binding peaks do not co-localize with peaks of H2Aub1, H2A.Z or +1 nucleosome. a and **c**, Venn diagrams showing the overlap between genes adjacent to the binding peaks of FLAG-RGA (current study) and H2Aub1 or H2A.Z (published ChIP-seq datasets). **b**, Genome-wide relative enrichment of RGA vs H2Aub1 binding peaks among the 1558 overlapping genes identified in **a**. **d**, Genome-wide relative enrichment of RGA vs H2A.Z binding peaks among the 2062 overlapping genes identified in **c**. **e**, RGA binding peak does not co-localize with +1 nucleosome. Top panel, Metagene plots showing nucleosome positioning in –1 kb to + 1 kb regions around TSS (using published MNase-seq dataset). Bottom panel, Genome-wide relative enrichment of RGA binding peaks in –1 kb to + 1 kb regions around TSS.

Supplementary Figure 10

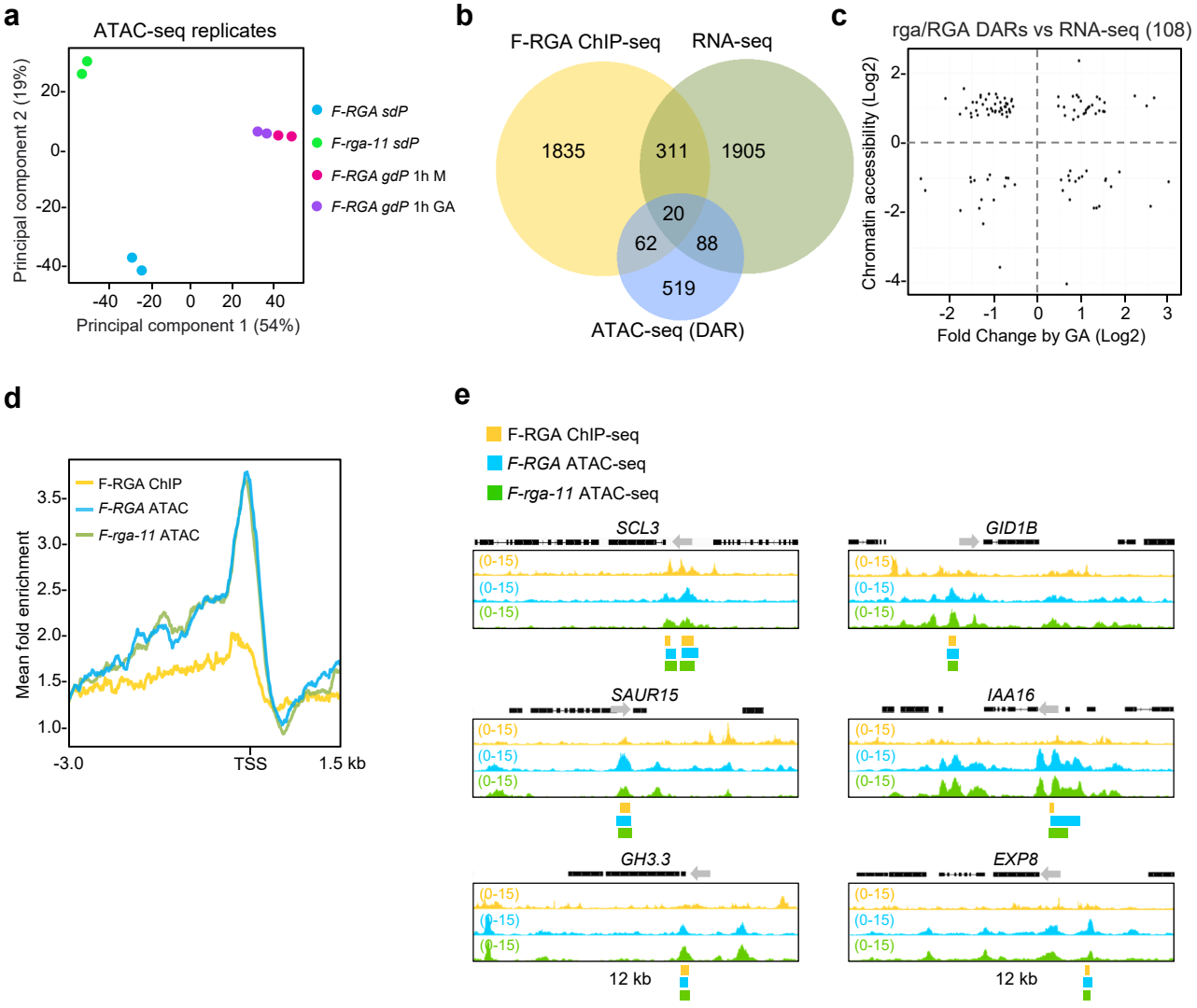

Supplementary Figure 10. Relative chromosome accessibility in *FLAG-RGA* and *FLAG-rga-11* (in *sly1 dP* background) by ATAC-seq. a, PCA analysis of 2 biological replicates of ATAC-seq experiment using *F-RGA sly1 dP, F-rga-11 sly1 dP*, *F-RGA ga1 dP* (1h mock) and *F-RGA ga1 dP* (1mM GA_4 for 1h). **b**, Venn diagram showing the overlap among genes adjacent to the binding sites of FLAG-RGA (this study), GA-responsive genes from RNA-seq, and DARs from *F-rga-11*/*F-RGA* ATAC-seq (this study). We did not include *F-RGA ga1 dP* (1h mock) and *F-RGA ga1 dP* (1h GA) in further data analysis because comparison between these ATAC-seq samples did not identify any DAR **c**, No correlation between chromatin accessibility (*F-rga-11* vs *F-RGA*) and GA responsiveness. Scatter plot containing 108 genes that are near DARs (*F-rga-11*/*RGA* ATAC-seq) and are GA-responsive. **d**, Overall relative enrichment of F-RGA binding vs chromatin accessibility in *F-RGA* and in *F-rga-11*. The 311 RGA direct target genes that were absent in DARs in *F-rga-11*/*F-RGA* ATAC-seq were used in this analysis. **e**, Genome brows er views of F-RGA ChIP-seq binding vs. chromatin accessibility profiles at selected loci (12 kb region is shown in each panel). Gene structures and names are above each panel. Yellow bar below indicates F-RGA binding peaks. Blue and green bars below indicate accessibility ATAC-seq peaks in *F-RGA* and *F-rga-11* lines, respectively. The data range of y-axis is 0-15.

Supplementary Figure 11. Unprocessed gel blot images for Supplementary Figures 2, 4 and 8.

Original Western blots for Figure S2. Boxed areas indicate the lanes/protein bands shown in Figure S2a.

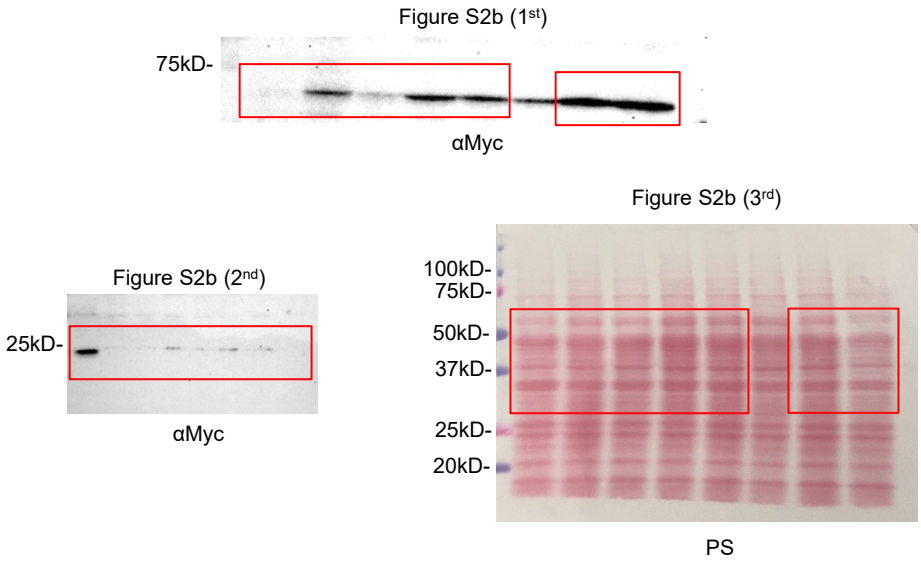

Original Western blots for Figure S2. Boxed areas indicate the lanes/protein bands shown in Figure S2b.

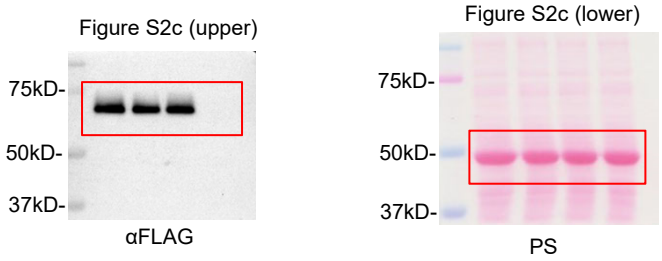

Original Western blots for Figure S2. Boxed areas indicate the lanes/protein bands shown in Figure S2c.

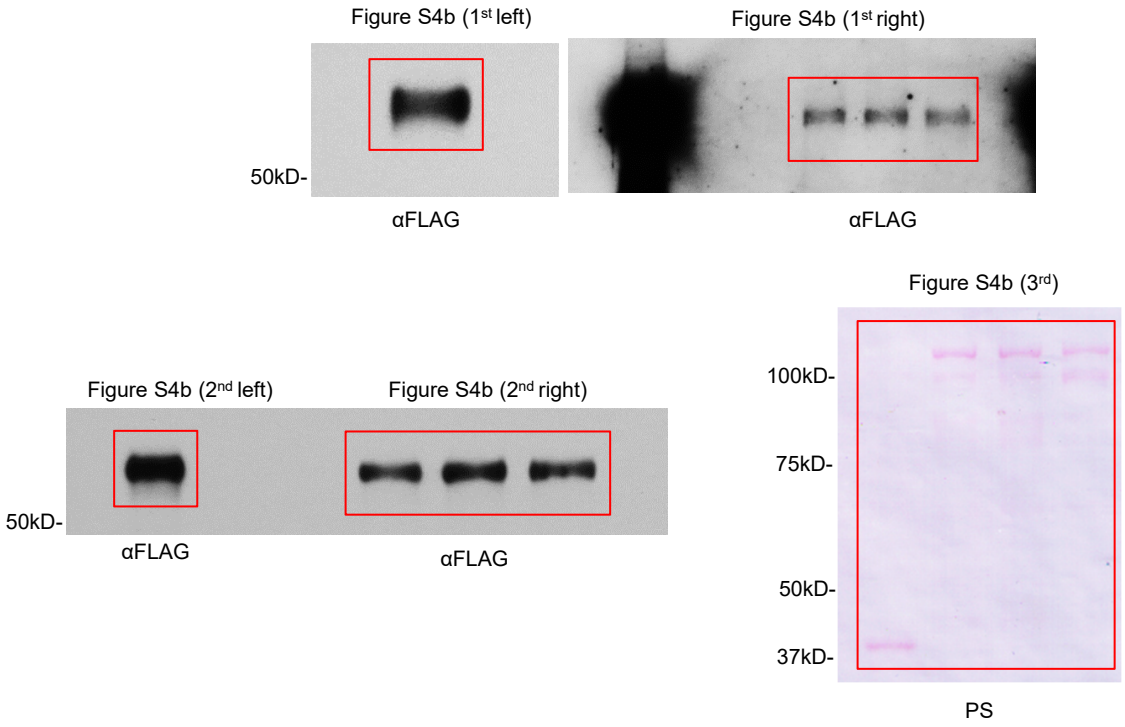

Original Western blots for Figure S4. Boxed areas indicate the lanes/protein bands shown in Figure S4b.

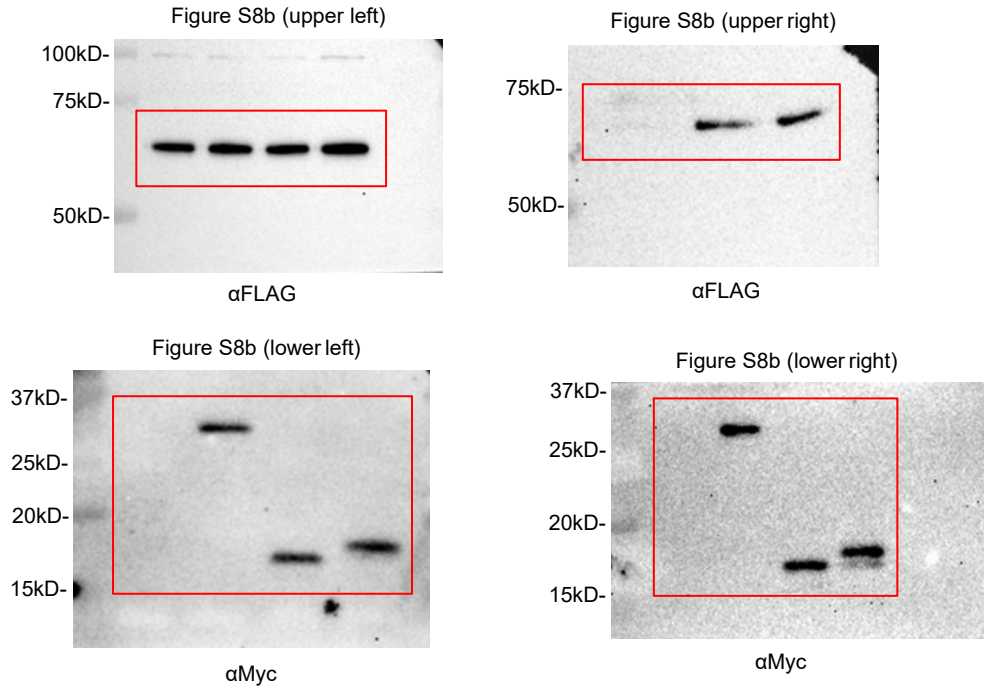

Original Western blots for Figure S8. Boxed areas indicate the lanes/protein bands shown in Figure S8b.